Rex's personal study notes

Rex

May 8, 2013

1 Graph basics

1.1 definitions

Gragh $G = (V, E)$ where V is the set of graph nodes and E is the set of edges that connect the nodes.

Incidence Matrix A 0-1 matrix which has V rows and E columns. $(v, e) = 1$ iff v is incident upon edge e. The incidence matrix ∇ of a graph and adjacency matrix A of its *line graph* are related by:

$$A = \nabla^T \nabla - 2I.$$

Laplacian Matrix , also called admittance matrix or Kirchhoff matrix, of a graph $G = (V, E)$ is an undirected, unweighted graph without graph loops (i, i) or multiple edges from one node to another. Its size is $n \times n$ ($n = |V|$) symmetric matrix defined by

$$L = D - A$$

where $D = diag(d_1, d_2, \ldots, d_n)$ is the degree matrix, and A is the adjacency matrix.

$$L = \nabla^T \nabla$$

normalized version of the Laplacian matrix is:

$$L^{norm}(G) = \begin{cases} 1 & \text{if } i = j \text{ and } d_j \neq 0 \\ -\frac{1}{\sqrt{d_i d_j}} & \text{if } i \text{ and } j \text{ are adjacent} \\ 0 & \text{otherwise} \end{cases}$$

or:

$$L^{norm}(G) = I - D^{-\frac{1}{2}} A D^{-\frac{1}{2}}$$

All eigenvalues of the normalized Laplacian are real and non-negative. If λ is an eigenvalue of L, then $0 \leq \lambda \leq 2$. These eigenvalues are the spectra of the normalized Laplacian.

1.2 Spectral Graph Theory

Spectral Theory for symmetric matrix: there exist n mutually orthogonal unit vectors $\psi_1, \psi_2, \ldots, \psi_n$ and numbers $\lambda_1, \lambda_2, \ldots, \lambda_n$ such that ψ_i is an eigenvector of eigenvallue λ_i.

Useful characterization: optimization of *Rayleigh quotient*:

$$\frac{x^T M x}{x^T x}$$

Easy to prove that if $x = \psi$, its Rayleigh quotient is λ.

Theorem 1.2.1. *The maximum vector that maximizes Rayleigh quotient is an eigenvector associated with the maximum eigenvalue. (Similar for minimum) (prove using matrix derivative)*

Isoperimetry and λ_2 The *isoperimetric ratio* of S, a sub-graph is:

$$\partial(S) \equiv (u, v) \in E : u \in S, v \notin S.$$

The *isoperimetric number* of a graph is the minimum isoperimetric number over all sets of at most half the vertices:

$$\theta_G \equiv \min_{|S| \leq n/2} \theta(S).$$

Lower bound on θ_G:

Theorem 1.2.2. *For every $S \subset V$, $\theta(S) \geq \lambda_2(1 - s)$, where $s = \frac{|S|}{|V|}$.*

The proof makes use of the characteristic vector of S,

$$\chi_S(u) = \begin{cases} 1 & \text{if } u \in S \\ 0 & \text{otherwise.} \end{cases}$$

1.3 Common Graphs

Lemma 1.3.1. *The Laplacian of K_n (complete graph) has eigenvalue 0 with multiplicity 1 and n with multiplicity $n - 1$. (check all vectors orthogonal to all-1s vector)*

Lemma 1.3.2. *v, w are vertices of degree one that are both connected to another vertex z. The vector ψ given by:*

$$\psi(u) = \begin{cases} 1 & u = v \\ -1 & u = w \\ 0 & \textit{otherwise.} \end{cases}$$

is an eigenvector of the Laplacian of G of eigenvalue 1.

Lemma 1.3.3. *The graph S_n (star graph) has eigenvalue 0 with multiplicity 1, eigenvalue 1 with multiplicity $n-2$ and eigenvalue n with multiplicity 1. (use previous lemma, and trace of a matrix equal to both sum of diagonal entries and eigenvalues)*

1.4 Graph Peoperties

Conductance In graph theory the conductance of a graph G=(V,E) measures how "well-knit" the graph is: it controls how fast a random walk on G converges to a uniform distribution. The conductance of a graph is often called the Cheeger constant of a graph as the analog of its counterpart in spectral geometry.

Small World Network A small-world network is a type of mathematical graph in which most nodes are not neighbors of one another, but most nodes can be reached from every other by a small number of hops or steps. Specifically, a small-world network is defined to be a network where the typical distance L between two randomly chosen nodes (the number of steps required) grows proportionally to the logarithm of the number of nodes N in the network.

$L \propto logN$

1.5 Basic operations

2 HCP : Tutorial

2.1 Concepts

A connectome is a comprehensive diagram of all neurons and synaptic connections contained within a nervous system.

2.2 About the project

This project aims to elucidate the neural pathways that underlie human brain function and behavior, which could shed light into the unique properties of human brains.
Four imaging modalities are used to acquire data:

1. functional MRI, diffusion MRI
2. Task-evoked fMRI
3. Structural MRI
4. Behavioral data

`http://www.humanconnectome.org/`

3 C-Elegans

Caenorhabditis elegans (pron.: /senrbdts lnz/) is a free-living, transparent nematode (roundworm).

- Size: about 1mm in length
- Number of neurons: It is one of the simplest organisms with a nervous system. In the hermaphrodite, this comprises 302 neurons whose pattern of connectivity, or "connectome", has been completely mapped and shown to be a small-world network.
- Number of synapses: 7000
- Sex: C-elegans has two sexes: hermaphrodites and males. Sex in C. elegans is based on an X0 sex-determination system.

  `http://worms.aecom.yu.edu/`

3.1 Clustering

To perform natural computation efficiently: specialized modules with locally dense connections

Significance of the existence of clusters: organization of functional modules.Ganglion vs. synaptic connection; Topological nature of the structure plays an important role in the information processing of C-elegans network.

C-elegans wiring 5 anatomical clusters in the C-elegans eonnectome, which correspond to experimentally-identified functional circuits. cooperation including mechanosensation, chemosensation and navigation

3.1.1 complex network analysis

Brain: small-world topology from microscopic level (eg. that of C-elegans) Scale-free degree distribution structural and functional motifs Robustness and fragility of brain structural networks with respect to lesions and diseases

Determination and characterization of hierarchical sluster structure: densely connected groups of nodes with sparser connections among groups Topological clusters in brain structure may correspond to sets of distinct anatomical modeules of neurons.

3.1.2 method

Modularity-based community detection algorithm for directed weighted networks. (modularity maximizatio approach)

Modularity is a quantitative measure defined as the number of edges falling within groups minus the expected number in an equivalent network with edges placed at random. The modularity value Q, indicates the degree to which a given paritition maximizes intra-cluster weights and minimizes inter-cluster weights.
Define: $Q = \frac{1}{4W} s^T (B + B^T) s$,
$B_{ij} = A_{ij} - \frac{S_i^{in} S_j^{out}}{W}$
B_{ij}: the extent to which the connections from j to i are prominent.
$W = \sum_{ij} A_{ij} = \sum_i S_i^{in} = \sum_i S_i^{out}$
Postive values demonstrate the possible presence of cluster structure.

Complexity : NP-complete; approximation heuristics to obtain a near-optimal community assignment vector. Constraints for C-elegans: information given by bilateral functional symmetry of the neuron cells. Simulated annealing method: a generic probabillistic metaheuristic for the global optimization problem of locating a good approximation to the global optimum of a given function in a large search space.

Prior knowledge: to reduce the number of community assignment vectors bilateral nuronal pairs have similar functional roles, accepting the principle of structure-function association in evolutionary biology.

Spectral detection; fast unfolding.

3.1.3 graph model

Degree: number of synaptic partner neurons of a neuron Weight: appropriate sum of synapses between specific neuronal partners Strength: total weights of synaptic connections afferent to or eferent from a neuron.

3.1.4 result

> While C. elegans neurons are spatially concentrated in a manner related to their ganglionic affiliation, we failed to observe a strong spatial localization of neurons belonging to the same cluster, except for those in clusters 11 and 12.

Hierarchical relationship of clusters is shown from the reordered adjacency matrix of C-elegans connectome.

Index of Qualitative Variation measures the diversity of types of ganglia in one cluster. 4 of 5 clusters did not display dominant neurotransmitter type. Low level of correlation between ganglia and cluster assignment.

Functional Cartography

- within-module weight
- participation coefficient

Characterize each neuron as either provincial or peripheral node, a hub, or a node with few within-module degrees. The types of nodes have a correlation with the types of neurons.

Use in Complex Behaviors Hub Cluster: outward synapses to clusters having many inward synapses; authoritative clusters have inward synapses from clusters that bridge to them through outward synapses.

> Thus, the body-spanning cluster 22, whose members are predominantly motor neurons, acted as an authority receiving information from hub clusters to produce consequential behaviors.
>
> the structural clusters indentified in this study appear to serve as a cohesive sub-module for information processing at various stages.

3.1.5 Present Constraints

- The lack of more appropriate model about inhibitory / excitatory sysnapses (some paper makes rough guess of the signs of synapses based on neurotransmitter gene expression data.)
- Directionality for gap junctions (even if it existed) cannot be extracted from electron micrographs.
- When a presynaptic terminal makes contact with two adjacent processes of different neurons, it is not known which of these processes acts as a postsynaptic terminal; both might be involved.

3.1.6 Ref

`web.mit.edu/lrv/www/elegans/` provides information about algorithmic approach to analyzing C-elegans neuronal network data. `www.wormatlas.org/ver1/MoW_built0.92/toc.html` structure of the nervous system of C-elegans

3.2 Spectral Analysis of C-elegans

Note There are 4 types of membrane regenerative potentials:

- Action potential
- Graded potential
- Intrinsic oscillation
- Plateau potential

The following papers disagree on the type of membrane potential that the neurons of C. elegans use: [10], [9], [8]. The last two articles are written by the same people: Shawn Lockery (University of Oregon) and Miriam Goodman (Stanford University).

Hodgkin-Huxley Equation is used to predict the quantitative behavior of a model nerve under a variety of conditions which corresponded to those in actual experiments. Their experiments show that the neuron cell membrane potential during an acitivity will rise from $-65mV$ to above $+40mV$ at the peak. This phenonmenon is explained by the changing permeability of different ions according to their voltage clamp experiment, which turns out to be an accurate electric model of neuron communication.

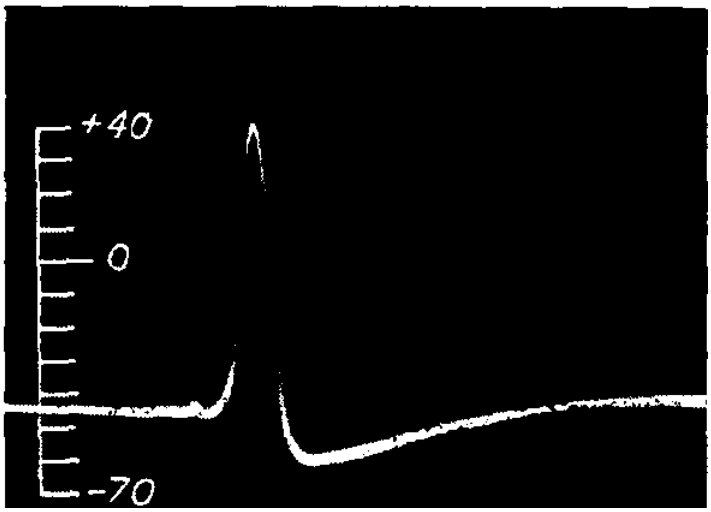

Figure 1: Action potential and resting potential recorded between inside and outside of axon with capillary filled with sea water. The sea water outside is treated as zero potential [3]

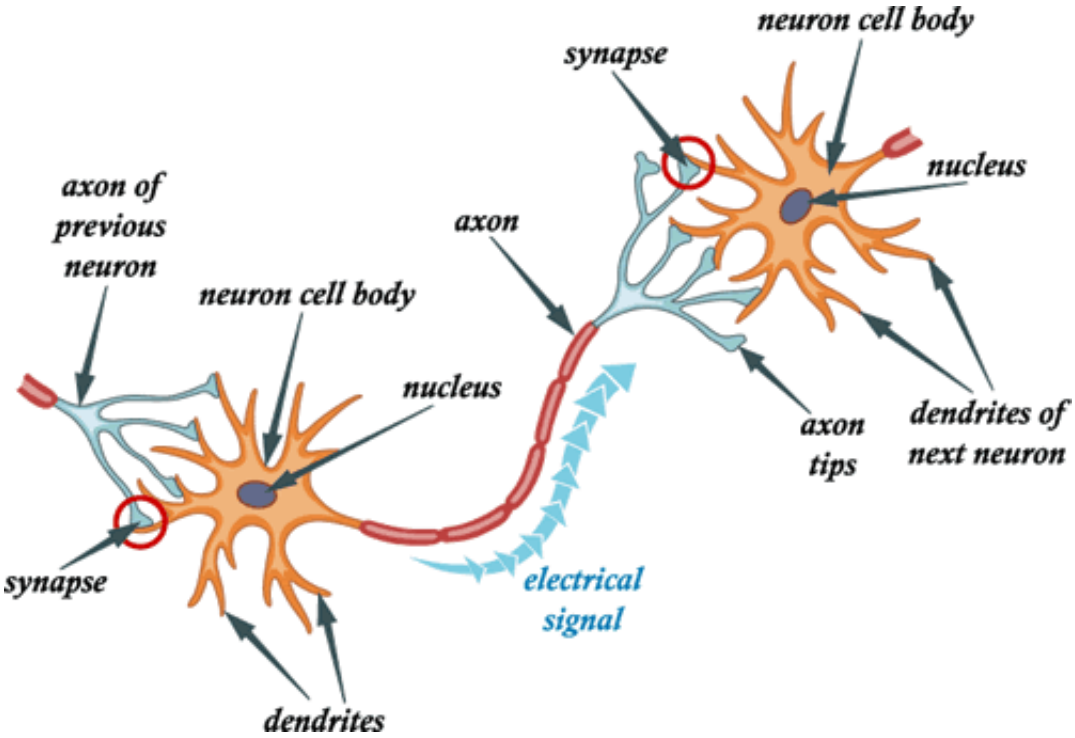

The following is my summery for the phases that the excitation of neurons goes through:

1. The firing threshold is reached. Action potential jumps high. There is influx of sodium ion through the ion channel.

2. Na^+ ion causes the membrane to be positively charged. Potassium ion starts to leave the cell(inhibitory factor).

3. Reaches peak in action potential. Sodium channels becomes refractory, and no more sodium ion is allowed to enter.

4. Repolarizing phase, when sodium ion channel still in its refractory phase, while potassium ions continues to leave the cell.

5. Potassium channels close. Sodium channel ends the refractory phase and reset to resting state.

6. Diffusion of extracellular potassium from cell causes in very slight increase in membrane voltage. (before resting, the cell is in **hyper-polarizing state**, the cell is not available for the next stimulation.

An illustration of various phases:

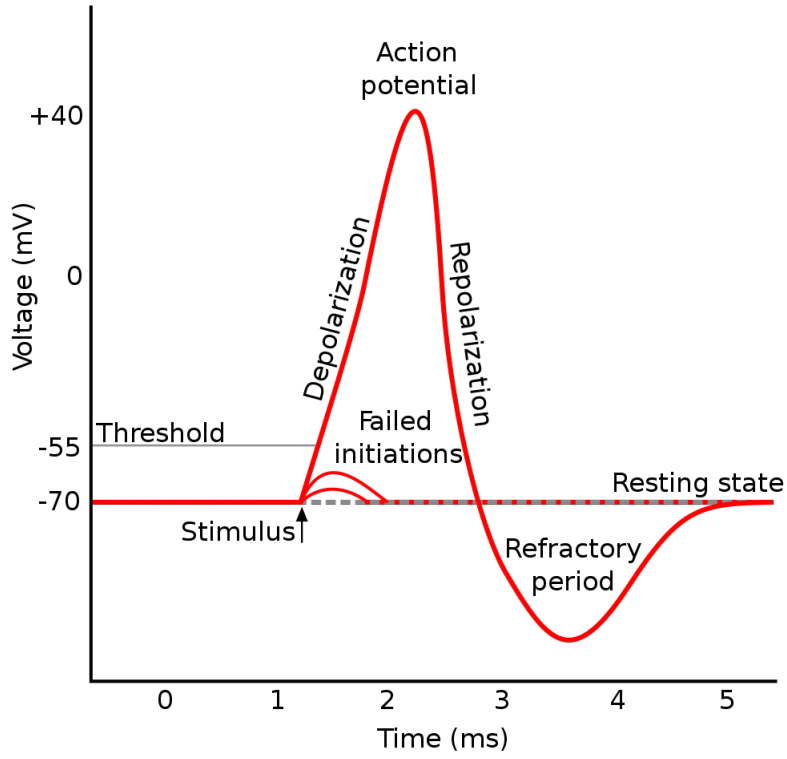

3.2.1 Mathematical model

Model for single cell:

$$C_m \frac{dV_m}{dt} + I_{ion} = I.$$

Where C_m denotes membrane capacitance per unit area; V_m the displacement of the membrane potential from its resting value (depolarization negative); t the time, I_{ion} the net ion current flowing accross the membrane (inward current positive), and I the total ion current density (inward current positive).

The I_{ion} can be further split into 3 components:

$$I_{ion} = I_{Na} + I_K + I_l, \begin{cases} I_{Na} = g_{Na}(E - E_{Na}), \\ I_K = g_K(E - E_K), \\ I_l = \bar{g}_l. \end{cases}$$

The leakage current I_l is caused by other ions such as Cl^-. E_{Na} and E_K are the equilibrium potentials for Na^+ and K^+.

The movement of ions is proportional to conductance times driving force. Let

$$\begin{cases} V = E - E_r, \\ V_{Na} = E_{Na} - E_r, \\ V_K = E_K - E_r, \\ V_l = E_l - E_r. \end{cases}$$

The Es can be replaced by Vs with respect to resting potential.

Ion channels for different ions contains many gates. If all gates are in permissive state, the channel is considered to be open, and ions are able to go through. The probability of a gate being in permissive state depends on the current value of the membrane voltage. HH model the gates as their probability of being in permissive state, ie. m, n, and h. The model specifies the number of gates each ion channel has:

$$I_{ion} = \bar{g}_{Na} m^3 h (V - V_{Na}) + \bar{g}_K n^4 (V - V_K) + \bar{g}_l (V - Vl),$$

where

$$\frac{dn}{dt} = \alpha_n (1 - n) - \beta_n n,$$
$$\frac{dm}{dt} = \alpha_m (1 - m) - \beta_m m,$$
$$\frac{dh}{dt} = \alpha_h (1 - h) - \beta_h h.$$

and

$$\alpha_n = \frac{0.01(V + 10)}{exp\frac{V+10}{10} - 1},$$
$$\beta_n = 0.125 exp\frac{V}{80},$$
$$\alpha_m = \frac{0.1(V + 25)}{exp\frac{V+25}{10} - 1},$$
$$\beta_m = 4 exp\frac{V}{18},$$
$$\alpha_h = 0.07 exp\frac{V}{20}$$
$$\beta_h = \frac{1}{exp\frac{V+30}{10} + 1}.$$

The above number and type of gates for each channel was determined using a trial-and-error method to find the order of gates to achieve the sigmoidal conductance found from previous results. The best match is the power of 4. The rate constants are obtained by fitting conductance data:

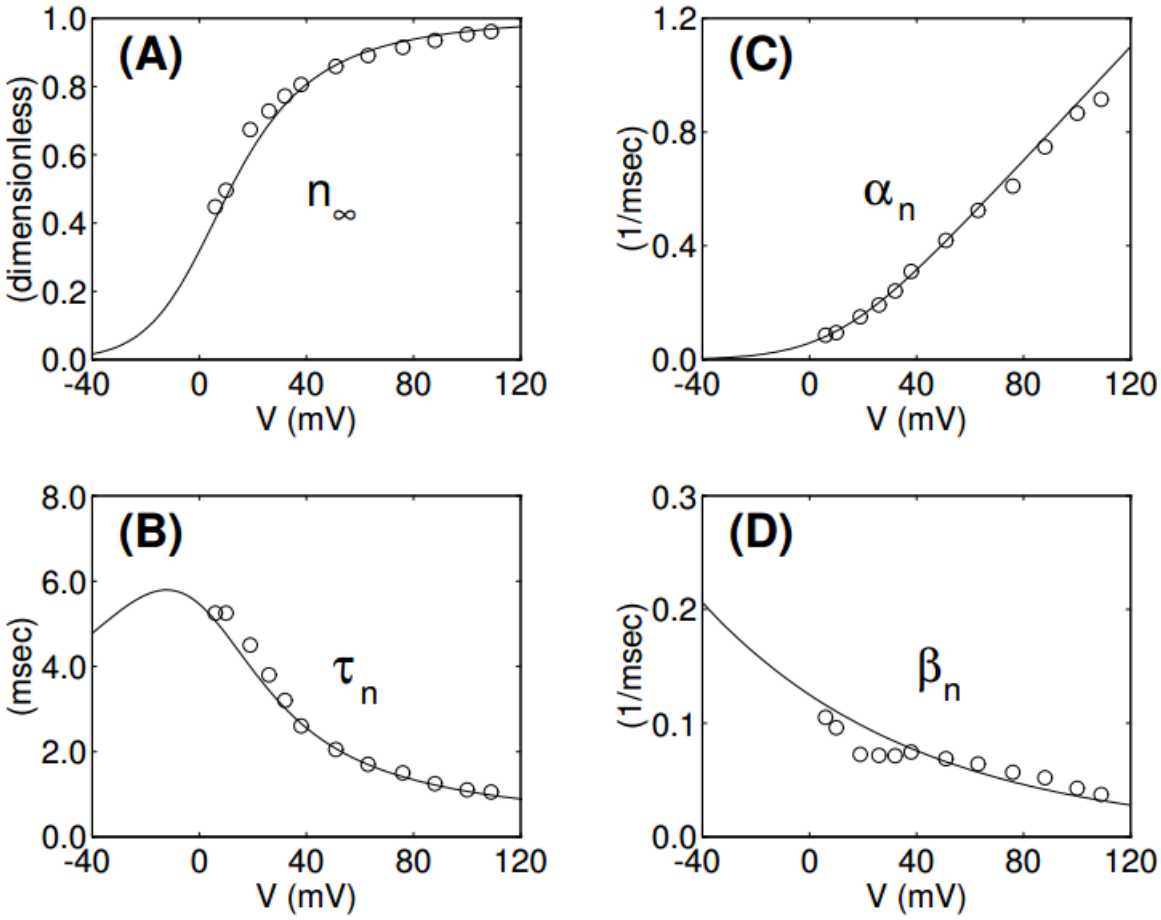

3.2.2 Simplification of HH Equation

FitzHugh-Nagumo Model:

$$\dot{V} = V - \frac{V^3}{3} - W + I$$

$$\dot{W} = 0.08(V + 0.7 - 0.8W)$$

3.3 Touch Circuit of C. elegans

Any such kind of complete circuit would consists of neurons from all 3 categories: sensory neuron, interneuron and motor neuron in order to facilitate an observable and meaningful behavior.

The touch circuit is identified in Chalfie et al. [1], using laser ablation techniques to kill the precursors of the neuron cells (mostly in embryos except AVM) and observe its effect on the touch sensitivity of C. elegans.

3.3.1 Classification

Sensory input There are 6 touch receptor cells:

- *ALMR, ALML*: anterior lateral microtubule cells. They are required for a full response to touch on the head.
- *PLMR, PLML*: posterior lateral microtubule cells. They are required for any response to touch on the tail.

- *AVM*: anterior ventral microtubule cell. AVM alone mediates a very weak touch response to head touch.
- *PVM*: posterior ventral microtubule cell. PVM alone does not mediate a detectable touch response.

Motor output Sets (coupled by gap junctions) of ventral cord motor neurons are responsible for muscle cell activity: [14]

- *A motor neurons* (12 VA cells and 9 DA cells)
- *B motor neurons* (11 VBs and 7 DBs)
- *D motor neurons* (13 VDs and 6 DDs)
- *11 AS motor neurons* share many of the properties of the DA cells

A and B neuron cells mediate muscle contraction for backward and forward movement (excitatory), and D cells mediate contralateral inhibition.

From Chalfie et al. [1], but there is no mention of whether all the A, B, D, AS neurons involve in touch response behavior.

3.3.2 Data

From the synapsis data, only 4 pairs of interneurons AVA, AVB, PVC, AVD synapse onto the motor neurons of the ventral cord and span the full length of the cord. They form synapses with touch cells in an interestingly complementary pattern:

Interneurons	Synapses made by	
	Anterior touch receptors	Posterior touch receptors
AVA	-	chemical
AVB	chemical(only AVM)	-
PVC	chemical	gap
AVD	gap	chemical

3.3.3 Testing

Speculation Is there a relationship between the multiplicity and type of synapses and the effectiveness of that neuron pathway.

Example (Chalfie et al. Figure 4):

The figure below shows that the anterior touch cells (ALM [1]) make EJ with AVA and AVD, and CJ with PVC; posterior touch cells (PLM) make EJ with PVC, and Chemical with AVD. The laser ablation experiment shows that AVA and AVD has no effect on anterior sensitivity, and PVC has no effect on posterior sensitivity. Hence it seems that the gap junction synapses between sensory and interneurons are more important in this touch circuit.

In contrast, the chemical synapses seem to play an inhibitory role. For example, the Chemical from ALM/AVM to PVC seems to inhibit the neuron signal to be propagated to B motor neurons, which will cause an inappropriate response.

Data fitting might be able to model the effectiveness of signal propagation in these circuits. In addition to setting a τ for weight (multiplicity), the type of synapses could also be taken into account.

Also, lots of connections such as the reciprocal synapses between AVA and PVC are not explained fully in terms of neurology. They might enable/inhibit certain pathways for certain behavior to be effective. (eg. reaction time)

[1] AVM not developed in young larvae with which this experiment is carried out

Rewiring It seems to me that rewiring could occur as adaptation for C elegans. For C elegans in postembryonic stage, when AVD is killed, they regain some touch sensitivity after a few more touches, which suggest that the Chemical between AVM-AVB-AVA-AVD [2] might act as an alternative pathway, which is not the optimum, but might be in use when the optimum path is damaged.

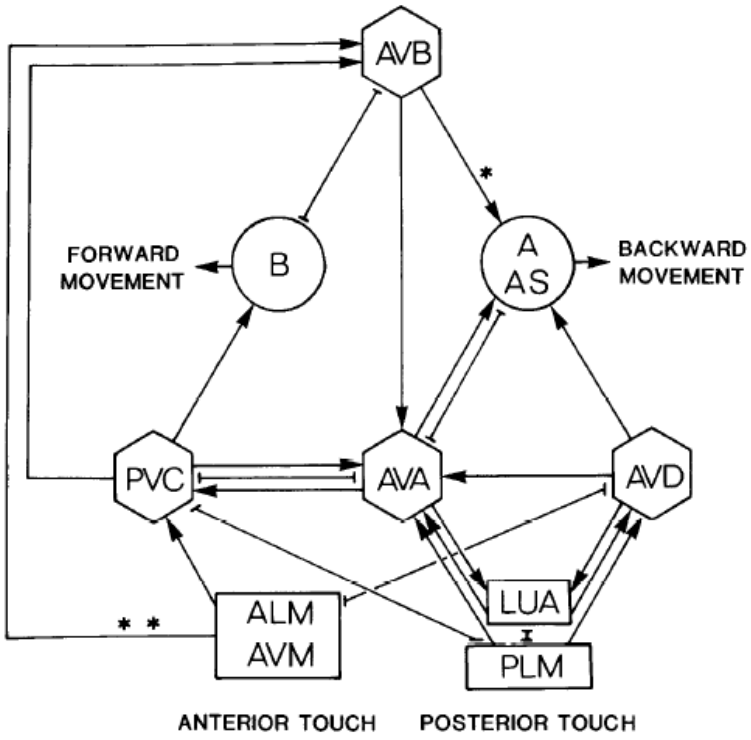

Figure 4. Neural circuitry for touch-induced movement. The touch cells and the touch cell connector, *LUA*, are designated by *rectangles*, the interneurons are designated by *hexagons*, and the motor neurons are designated by *circles*. Both chemical synapses (⟶) and gap junctions (⟝) are indicated. The diagram represents a composite of data and does not indicate the changes that occur in the circuitry during development; e.g., the connections from *AVM* to *AVB* are formed late in larval development. Missing from the diagram are the gap junctions between identical motor neurons and interneurons and the gap junctions joining *AVM* and *ALM*. *AVB* forms chemical synapses only with the *AS* cells, not the *A* cells (*); only *AVM* of the anterior touch cells chemically synapses onto *AVB* (**). The connections made by the interneurons are taken from White et al., (1976; J. G. White, E. Southgate, J. N. Thomson, and S. Brenner, unpublished data).

The following table illustrates the result of disabling certain interneuron(s):

Interneurons killed	Sensitive at head		Sensitive at tail		Forward movement	Backward movement
	Larva	Adult	Larva	Adult		
PVC	✓	✓	-	-	✓	✓
AVD	-	✓(adapted)	✓	✓	✓	✓
AVD, AVM	-	-	✓	✓	✓	✓
AVA	✓	✓	✓	✓	✓	uncoordinated [3]
AVA, AVD	-	✓[4]	✓	✓	✓	-
AVB	✓	✓	✓	✓	uncoordinated	✓
AVB, PVC	✓	✓	-	-	- [5]	✓

3.4 Other functional circuits suggested

All these circuits could be the biological ground truth for doing clustering. Checking 1D eigenspace would be simple. 3D needs more thoughts.

[2] from experimental results AVA seems to be important in this alternative pathway

Figure 2: Learned NaCl Aversion. Based on data from Hukema et al.(2006), Tomioka et al. (2006), Fu et al. (2009), Kano et al. (2008), Ishihara et al. (2002), and White et al. (1986)

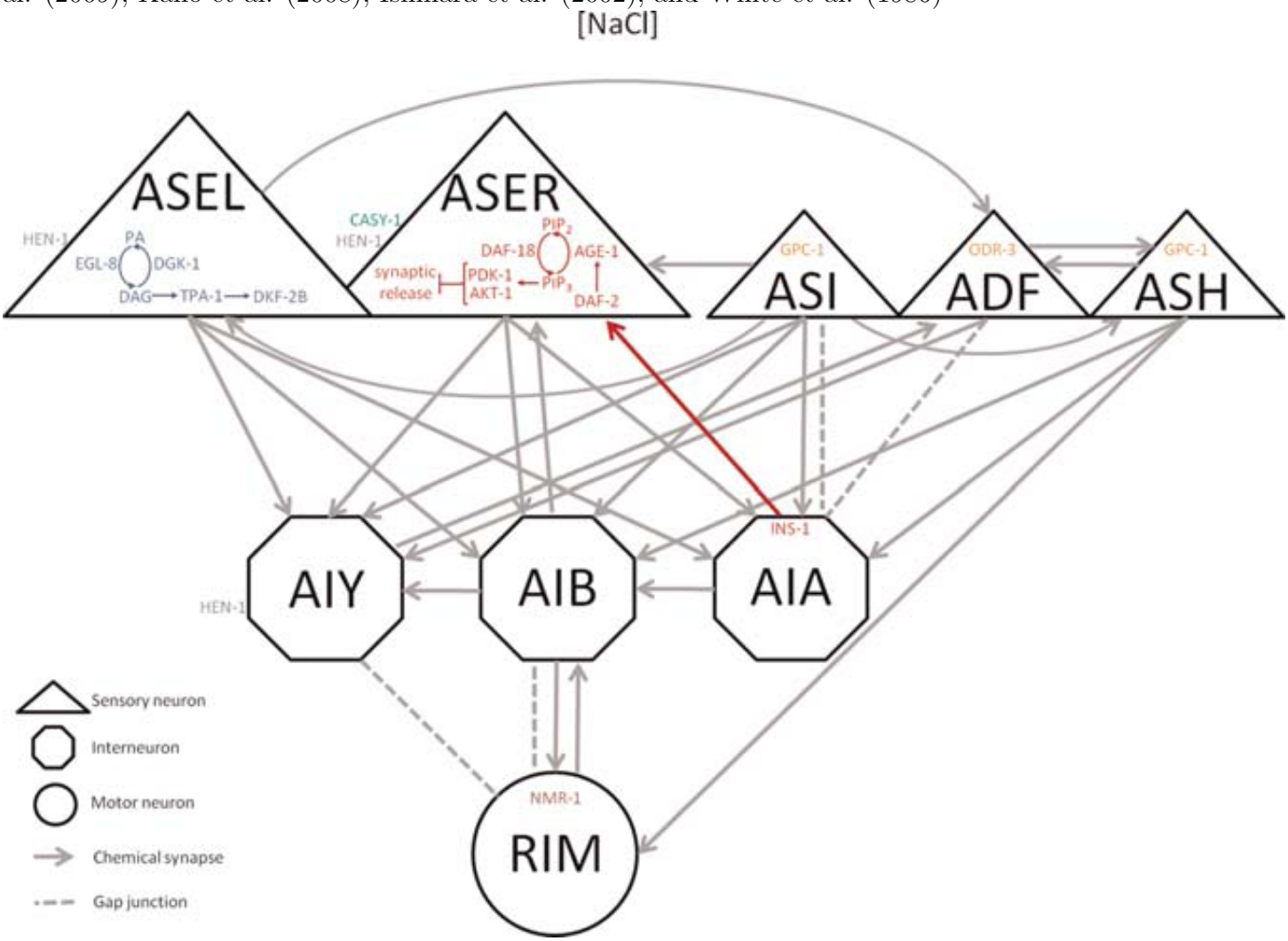

Electrosensory Behavior [2] It is the biological ability to perceive natural electrical stimuli. The following diagram is not considered as comprehensive, but the author did suggest why interneurons such as AIY are not significant in electrosensory neural circuits according to the experiments.

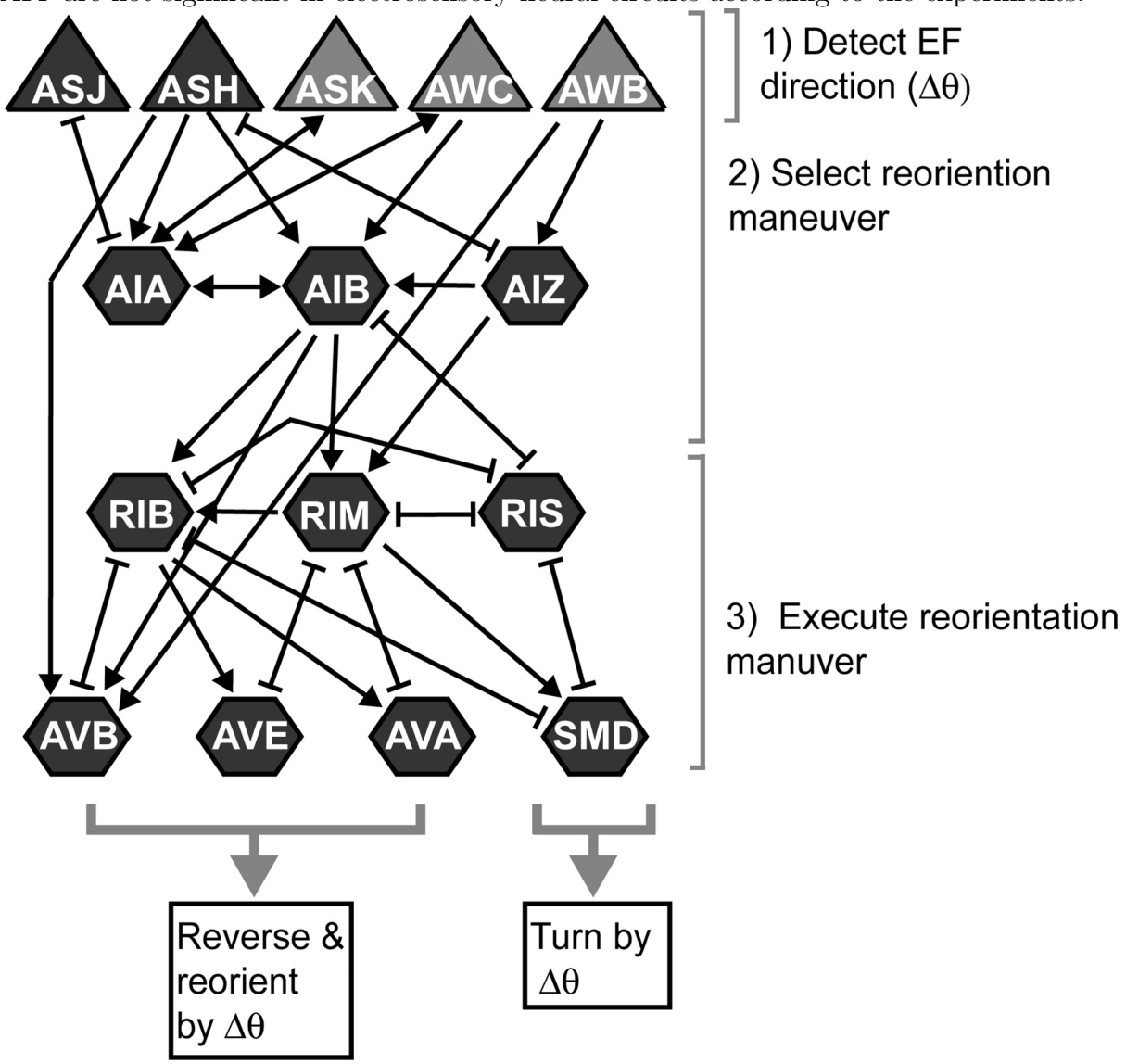

Figure 3: Neural circuits for electrosensory behavior. The wiring diagram of neural pathways that might contribute to electrosensory behavior is shown. Synaptic connections between neurons follow the wiring diagram established by White et al. (1986). Sensory neurons are indicated by red triangles. Interneurons and command motor neurons are indicated by hexagons. Chemical synaptic connections between neurons are indicated by arrows. Gap junctions are indicated by brackets. We suggest that the primary neurons for electrosensory detection are ASJ and ASH. RIM and AVA appear contribute to turns and reversals during electrosensory steering, respectively. Additional neurons show pathways that might connect ASJ, ASH, RIM, and AVA to motor output during electrosensory behavior, as well as several other neurons that have been implicated in the execution of turns and reversals during exploratory behaviors (Tsalik and Hobert, 2003; Wakabayashi et al., 2004; Gray et al., 2005). EF, Electric field. sed on data from Hukema et al.(2006), Tomioka et al. (2006), Fu et al. (2009), Kano et al. (2008), Ishihara et al. (2002), and White et al. (1986)

3.5 June 18 2013 Work Notes

Parsing of hermaphrodite C. elegans neuron connection.

Read neuron connect data from a csv file converted from an excel file "NeuronConnect" downloaded from 2.1 of `http://www.wormatlas.org/neuronalwiring.html` ([13]).
script file name: Run_parseHermConnectome.m.

Figure 1 : sparse graph of electric junction visualization.

Figure 2 and 3 : degree/strength plot in descending order. Max degree: 40; max nodal strength: 113.

Figure 4 : Survival Function for degrees of gap junction network. In real world, there is often noise present at the tail of the degree distribution: the degree distribution has a long right tail of values that are far above the mean. One method to get arround the problem is to construct a histogram in which the bin sizes increase exponentially with degree (number of samples in each bin is divided by the width of the bin to normalize measurement); the other way is to use CDF/survival function (the advantage is there is no loss of information). (in order to check Power-law Degree Distributions).

Figure 5 : Histogram of Path Length for Herm Gap Junction Network (weighted). The shortest path computation is done using bioinformatics toolbox (Johnson Algorithm). Average path length is also calculated.

Other measures : Jaccard Coefficient, Cluster Coefficient

Figure 6 : sparse graph of Chemical junction visualization.

3.5.1 Centrality

Various measures of centrality are used to determine the relative importance of a vertex within the graph.

Degree Centrality is defined as the number of links incident upon a node. In the case of directed graph, indegree and outdegree centrality values are calculated. (Definition can be extended to evaluate centrality of graph)

Closeness Centrality of a node is its total distance to all other nodes. The smaller the value, the more central is the node.

Betweenness Centrality of a vertex within a graph quantifies the number of times a node acts as a bridge along the shortest path between two other nodes. Vertices that have a high probability to occur on a randomly chosen shortest path between two randomly chosen vertices have a high betweenness.

$$C_B(v) = \sum_{s \neq v \neq t \in V} \frac{\sigma_{st}(v)}{\sigma_{st}}$$

Algorithm to compute betweenness of a vertex v in a graph $G = (V, E)$:

- For each pair of vertices (s, t), compute the shortest path between them
- For each pair of vertices (s, t), determine the fraction of shortest paths that pass through vertex v
- Sum this fraction over all pairs of vertices (s, t)

Eigenvector Centrality uses the eigenvector that corresponds to the greatest eigenvector of the adjacency matrix of the graph x to determin the influence of a node. The score of each node is x_i, based on the concept that connections to high-scoring nodes contribute more to the score of the node in question than equal connections to low-scoring nodes.

4 Male C-elegans Wiring Data

Male C. elegans has 81 neurons in addition to hermaphrodite C. Elegans. [5]

More info: The six most central neurons are: AVAL, AVBR, RIGL, AVBL, RIBL and AVKL

Single combined network by adding the adjacency matrix of the gap junction and chemical networks together:

> New net work consisting 279 neurons and 2990 directed connections. It has one large strongly connected component of 274 neurons and 5 strongly isolated neurons. The 5 isolated neurons are IL2DL/R, PLNR, DD06, PVDR. Mean path length $L = 2.87$.

4.1 Neuron List

Table 1: NEURON LIST, C. ELEGANS ADULT MALE, N2Y SERIES AND CLUSTERING INFORMATION

Index	Neurons [6]	GS/MS [7]	Neuron type	Location [8]	Module [9]	Cluster [10]	Notes
1	ADAL	GS				11	
2	ADAR	GS				11	
3	ADEL	GS				13	
4	ADER	GS				13	
5	ADFL	GS				11	
6	ADFR	GS				11	
7	ADLL	GS				11	
8	ADLR	GS				11	
9	AFDL	GS				11	
10	AFDR	GS				11	
11	AIAL	GS				11	
12	AIAR	GS				11	
13	AIBL	GS				11	
14	AIBR	GS				11	
15	AIML	GS				11	
16	AIMR	GS				11	
17	AINL	GS				11	
18	AINR	GS				11	
19	AIYL	GS				11	
20	AIYR	GS				11	
21	AIZL	GS				11	
22	AIZR	GS				11	
23	ALA	GS				12	
24	ALML	GS				21	
25	ALMR	GS				21	
26	ALNL	GS	sensory neuron	tail - left lumbar ganglion	N/A	11	Partial reconstr
27	ALNR	GS	sensory neuron	tail - right lumbar ganglion	N/A	11	Partial reconstr
28	AN1a [11]	GS	interneuron	head - lateral / retrovesicular ganglion		22	AVF,AVH,AVJ
29	AN1b [12]	GS	interneuron	head - lateral / retrovesicular ganglion		22	AVF,AVH,AVJ

[6]Link to map, synapse lists, circuit diagrams. Standardized: [5]

[7]gender shared (GS) or male-specific (MS)

[8]Location of cell body

[9]Cluster according to [5]. There are in total 5 clusters named as: Response, Locomotion, R(1-5)A, PVV, Insemination Module

[10]Cluster according to [12]. There are in total 5 clusters named as: 11, 12, 13, 21, 22

[11]a.k.a. AVFL

[12]a.k.a. AVFR

30	AN2a [13]	GS	interneuron	Head - lateral / retrovesicular ganglion		22	AVF,AVH,AVJ
31	AN2b [14]	GS	interneuron	head - lateral / retrovesicular ganglion		22	AVF,AVH,AVJ
32	AN3a [15]	GS	interneuron	head - lateral / retrovesicular ganglion	PVV	21	AVF,AVH,AVJ R1BR
33	AN3B [16]	GS	interneuron	head - lateral / retrovesicular ganglion	PVV	21	AVF,AVH,AVJ R5BR
34	AQR	GS				13	
35	AS01	GS				21	
36	AS02	GS				22	
37	AS03	GS				22	
38	AS04	GS				22	
39	AS05	GS				22	
40	AS06	GS				22	
41	AS08	GS	motor neuron	tail - ventral cord	Locomotion	21	Ventral portion tions with, and
42	AS09	GS	motor neuron	tail - ventral cord	Locomotion	21	Ventral portion tions with, and
43	AS10	GS	motor neuron	tail - preanal ganglion	Locomotion	21	Ventral portion tions with, and
44	AS11	GS	motor neuron	tail - preanal ganglion	PVV	21	Postsynaptic to to VD13 and b
45	ASEL	GS				11	
46	ASER	GS				11	
47	ASGL	GS				11	
48	ASGR	GS				11	
49	ASHL	GS				11	
50	ASHR	GS				11	
51	ASEL	GS				11	
52	ASEL	GS				11	
53	ASEL	GS				11	
54	ASEL	GS				11	
55	ASEL	GS				11	
56	ASEL	GS				11	
57	ASEL	GS				11	
58	ASEL	GS				11	
59	AVAL	GS	interneuron	head - left lateral ganglion	Locomotion	21	Command inte type body wall put from PQR, neurons

[13] a.k.a. AVHL
[14] a.k.a. AVHR
[15] a.k.a. AVJL
[16] a.k.a. AVJR

60	AVAR	GS	interneuron	head - right lateral ganglion	**Locomotion**	**21**	Command inte type body wall from PQR, out
61	AVBL	GS	interneuron	head - left lateral ganglion	**Locomotion**	**21**	Command inte type body wall from AVA
62	AVBR	GS	interneuron	head - right lateral ganglion	**Response**	**21**	Command inte type body wall from MS intern
63	AVDL	GS	interneuron	head - left lateral ganglion	**Locomotion**	**21**	Command inte presynaptic to,
64	AVDR	GS	interneuron	head - right lateral ganglion	**Locomotion**	**21**	Command inte presynaptic to,
65	AVG	GS	interneuron	head - retrovesicular ganglion	**Response**	**21**	Guidepost inte and LUA.
66	AVKL	GS	interneuron	head - left ventral ganglion		**13**	Makes gap jun PDER
67	AVKR	GS	interneuron	head - right ventral ganglion		**13**	Runs on left si tions with hypo
68	AVL	GS	interneuron	head - right ventral ganglion	**Insemination**	**13**	Makes gap junc and ventral boo
69	CA02	MS	interneuron	tail - ventral cord	**Insemination**		Uncertain cell I
70	CA03	MS	interneuron	tail - ventral cord	**Insemination**		Uncertain cell I
71	CA04	MS	interneuron	tail - ventral cord	**PVV**		Uncertain cell ganglion. Make from Ray neuro
72	CA05	MS	interneuron	tail - ventral cord	**Insemination**		Makes many ga sensory neurons
73	CA06	MS	interneuron	tail - ventral cord	**Insemination**		Posteriorly dire anal ganglion, right cloacal co tions with CA0 cess from cell b nation of this p
74	CA07	MS	interneuron	tail - ventral cord	**Response**		Process from sure. Unbranch synapses
75	CA08	MS	interneuron	tail - preanal ganglion	**Locomotion**		Process from c Anteriorily dire and ventral boo
76	CA09	MS	interneuron	tail - preanal ganglion	**R(1-5)A**		Extensive bran from cell body I of this process
77	CP01	MS	interneuron	tail - ventral cord	**Insemination**		Uncertain cell I junctions with
78	CP02	MS	interneuron	tail - ventral cord	**Insemination**		Uncertain cell I junctions with HOB

79	CP03	MS	interneuron	tail - ventral cord	**Insemination**		Uncertain cell with body wall muscles.
80	CP04	MS	interneuron	tail - ventral cord	**Insemination**		Unbranched pr NMJs with bod
81	CP05	MS	interneuron	tail - ventral cord	**Insemination**		Innervates the
82	CP06	MS	interneuron	tail - ventral cord	**Insemination**		Innervates the
83	CP07	MS	interneuron	tail - ventral cord	**PVV**		Several branche with Ray 7 neu
84	CP08	MS	interneuron	tail - preanal ganglion	**PVV**		Highly branche with Ray 7 neu
85	CP09	MS	interneuron	tail - preanal ganglion	**PVV**		Highly branche with Ray 6 neu
86	DA04	GS	motor neuron	tail - ventral cord	**Response**	**22**	Uncertain cell I tion
87	DA05	GS	motor neuron	tail - ventral cord	**Locomotion**	**22**	Uncertain cell I tion
88	DA06	GS	motor neuron	tail - ventral cord	**Locomotion**	**21**	Ventral portion tions with, and
89	DA07	GS	motor neuron	tail - ventral cord	**Locomotion**	**21**	Ventral portion tions with, and
90	DA08	GS	motor neuron	tail - ventral cord	**Locomotion**	**21**	Makes gap junc naptic to D-typ in dorsal cord
91	DA09	GS	motor neuron	tail - ventral cord	**Locomotion**	**21**	Makes gap junc in ventral cord. cord
92	DB03	GS	motor neuron	tail - ventral cord		**22**	Uncertain cell I tion
93	DB04	GS	motor neuron	tail - ventral cord	**Locomotion**	**22**	Uncertain cell I tion
94	DB05	GS	motor neuron	tail - ventral cord	**Locomotion**	**21**	Uncertain cell I tion
95	DB06	GS	motor neuron	tail - ventral cord	**Locomotion**	**21**	Ventral portion tions with AVI and interneuron
96	DB07	GS	motor neuron	tail - preanal ganglion	**Locomotion**	**21**	Ventral portion tions with AVE
97	DD03	GS	motor neuron	tail - ventral cord	**Locomotion**	**22**	Uncertain cell I tion
98	DD04	GS	motor neuron	tail - ventral cord	**Locomotion**	**22**	Ventral portion tions with VD type motor neu
99	DD05	GS	motor neuron	tail - ventral cord	**Locomotion**	**22**	Ventral portion tions with PVZ and VB motor
100	DD06	GS	motor neuron	tail - preanal ganglion	**Locomotion**	**21**	Ventral cord pro SPV, R2A and process makes

101	DVA	GS	interneuron	tail - dorsorectal ganglion		21	Makes gap junc postdeirid senso
102	DVB	GS	interneuron	tail - dorsorectal ganglion	Insemination	21	Makes NMJs w
103	DVC	GS	interneuron	tail - dorsorectal ganglion	Locomotion	13	Makes gap junc
104	DVE	MS	interneuron	tail - dorsorectal ganglion	Insemination	N/A	Presynaptic to
105	DVF	MS	interneuron	tail - dorsorectal ganglion	Insemination	N/A	Makes gap junc put to HOB an
106	DX1	MS	interneuron	tail - dorsorectal ganglion	Response	N/A	Makes few gap Input from HO glion
107	DX2	MS	interneuron	tail - dorsorectal ganglion	Insemination	N/A	Makes gap junc put from HOB ganglion
108	DX3	MS	interneuron	tail - dorsorectal ganglion	Response	N/A	Makes gap junc put from HOB.
109	EF1	MS	interneuron	tail - dorsorectal ganglion		N/A	Forms sheet-lik glion. Makes ga siderable input
110	EF2	MS	interneuron	tail - dorsorectal ganglion		N/A	Forms sheet-lik glion. Makes ga siderable input
111	EF3	MS	interneuron	tail - preanal ganglion		N/A	Forms sheet-lik glion. Makes ga siderable input
112	HOA	MS	sensory neuron	tail - preanal ganglion	Response	N/A	Very large cell ganglion. Mak and PCB. Pres synaptic to HO
113	HOB	MS	sensory neuron	tail - preanal ganglion	Insemination	N/A	Very large cell ganglion. Mak Presynaptic to
114	LUAL	GS	interneuron	tail - left lumbar ganglion	Response	21	Input from HO and multiple M
115	LUAR	GS	interneuron	tail - right lumbar ganglion	Response	21	Input from HO MS interneuron
116	PCAL	MS	sensory neuron	tail - left cloacal ganglion	Response	N/A	Makes gap junc put to PVX an
117	PCAR	MS	sensory neuron	tail - right cloacal ganglion	Response	N/A	Makes gap junc put to PVX an
118	PCBL	MS	sensory/motor neuron	tail - left cloacal ganglion	Insemination	N/A	Makes NMJs w cles. Makes ga from PCA
119	PCBR	MS	sensory/motor neuron	tail - right cloacal ganglion	Insemination	N/A	Makes NMJs w cles. Makes gap
120	PCCL	MS	sensory/motor neuron	tail - left cloacal ganglion	Insemination	N/A	Innervates the

121	PCCR	MS	sensory/motor neuron	tail - right cloacal ganglion		N/A	Innervates the muscle
122	PDA	GS	motor neuron	tail - preanal ganglion	PVV	21	Makes NMJs w
123	PDB	GS	interneuron	tail - preanal ganglion	PVV	21	Makes NMJs w sensory and int
124	PDC	MS	interneuron	tail - preanal ganglion	PVV	N/A	Makes NMJs w junctions with
125	PDEL	GS	sensory neuron	posterior half of body - left		21	Input/output w and AVK in th
126	PDER	GS	sensory neuron	posterior half of body - right		21	Input/output w and AVK in th
127	PGA	MS	interneuron	tail - preanal ganglion	PVV	N/A	Multiple "weak
128	PHAL	GS	sensory neuron	tail - left lumbar ganglion	Response	21	Makes gap junc put to EF3, PV
129	PHAR	GS	sensory neuron	tail - right lumbar ganglion	Response	21	Makes gap jun neurons. Outpu
130	PHBL	GS	sensory neuron	tail - left lumbar ganglion	Response	21	Makes gap jun R3B
131	PHBR	GS	sensory neuron	tail - right lumbar ganglion	Response	21	Makes gap junc R9B
132	PHCL	GS	sensory neuron	tail - left lumbar ganglion		21	Output to AVA
133	PHCR	GS	sensory neuron	tail - right lumbar ganglion		21	Output to AVA
134	PLML	GS	sensory neuron	tail - left lumbar ganglion		21	Ventral cord p Output to PDE
135	PLMR	GS	sensory neuron	tail - right lumbar ganglion		21	Ventral cord p Output to DVA
136	PLNL	GS	sensory neuron	tail - left lumbar ganglion		11	Some Ray neur
137	PLNR	GS	sensory neuron	tail - right lumbar ganglion		11	Some Ray neur
138	PQR	GS	sensory neuron	tail - left lumbar ganglion		21	Input from MS AVD
139	PVCL	GS	interneuron	tail - left lumbar ganglion	Locomotion	21	makes gap junc MS and GS (e motor neurons
140	PVCR	GS	interneuron	tail - right lumbar ganglion	Locomotion	21	makes gap junc MS and GS (e motor neurons
141	PVDL	GS	sensory neuron	posterior half of body - left		21	Output to AVA
142	PVDR	GS	sensory neuron	posterior half of body - right		21	Output to AVA
143	PVM	GS	sensory neuron	left - posterior half of body		21	Makes gap junc
144	PVNL	GS	interneuron	tail - left lumbar ganglion	Response	21	Input from Ray interneurons

145	PVNR	GS	interneuron	tail - right lumbar ganglion	PVV	21	Input from Ray
146	PVQL	GS	interneuron	tail - left lumbar ganglion		11	Extensively gap
147	PVQR	GS	interneuron	tail - right lumbar ganglion		11	Extensively gap
148	PVR	GS	interneuron	tail - right lumbar ganglion		21	Makes gap junc put to motor ne
149	PVS [17]	GS	interneuron	tail - preanal ganglion	PVV	13	Extensively gap Input from AN
150	PVT	GS	interneuron	tail - preanal ganglion	Insemination	13	Extensively gap
151	PVU [18]	GS	interneuron	tail - preanal ganglion	Locomotion	13	Makes gap junc
152	PVV	MS	interneuron	tail - preanal ganglion	PVV	N/A	Posteriorly-dire branchy and ve ray neurons. A ventral body w many other neu
153	PVWL	GS	interneuron	tail - left lumbar ganglion		21	Few synapses in
154	PVWR	GS	interneuron	tail - right lumbar ganglion		21	Few synapses in
155	PVX	MS	interneuron	tail - preanal ganglion	Response	N/A	Several branch LUA, phasmid Anteriorly-direc terneurons and
156	PVY	MS	interneuron	tail - preanal ganglion	Response	N/A	Few branches a and MS sensor motor neurons. near the hook
157	PVZ	MS	interneuron	tail - preanal ganglion	Response	N/A	Makes gap junc D-type motor n wall muscle an from hook sens
158	R1AL	MS	sensory neuron	tail - left lumbar ganglion	R(1-5)A	N/A	In the lumbar an anteriorly di each of which b tic branch. Co cess. Mainly po preanal ganglio Posteriorly-dire input/output w

[17] a.k.a. PVPR
[18] a.k.a. PVPL

159	R1AR	MS	sensory neuron	tail - right lumbar ganglion	**R(1-5)A**	N/A	In the lumbar g anteriorly direc the commisure from other Ra diagonal muscle In the preanal (presumably).
160	R1BL	MS	sensory neuron	tail - left lumbar ganglion	**PVV**	N/A	In the lumbar teriorly directe one posterior pr anterior process Ray neurons o ganglion: Ente R6BL, R3BL. with output to
161	R1BR	MS	sensory neuron	tail - right lumbar ganglion	**PVV**	N/A	In the lumbar an anteriorly d with the distal the commissure preanal ganglio DD6. Long po branches at the RayB neurons
162	R2AL	MS	sensory neuron	tail - left lumbar ganglion	**R(1-5)A**	N/A	In the lumbar g directed proces end of the ant sure. Input/out NMJs with boo anterior process commissure alo directed proces Main input/out
163	R2AR	MS	sensory neuron	tail - right lumbar ganglion	**R(1-5)A**	N/A	In the lumbar orly directed p distal end of th missure. Input Posterior portio tion makes NM preanal ganglio DD6, then split a posteriorly d input/output w
164	R2BL	MS	sensory neuron	tail - left lumbar ganglion	**Response**	N/A	In the lumbar g cess emanates sure proximal t In the preanal then splits into and a posterior with LUAL. Al

165	R2BR	MS	sensory neuron	tail - right lumbar ganglion	**Response**	N/A	In the lumbar g cess emanates sure proximal R3AR. In the p with R7AR, R4 rected process furcations. Ma output to LUA
166	R3AL	MS	sensory neuron	tail - left lumbar ganglion	**R(1-5)A**	N/A	In the lumbar an anteriorly d with the distal the commissure the cell body. commissure. In missure with R directed proces put/output wit
167	R3AR	MS	sensory neuron	tail - right lumbar ganglion	**R(1-5)A**	N/A	In the lumbar an anteriorly d with the distal the commissure cell body. Exte missure. In th missure with R process with a with R3AL and
168	R3BL	MS	sensory neuron	tail - left lumbar ganglion	**PVV**	N/A	In the lumbar g anteriorly direc the the distal e the commissure the CB, which input/output w In the preanal R3AL, R5AL, R forms many spi on the right sid Main output to
169	R3BR	MS	sensory neuron	tail - right lumbar ganglion	**Response**	N/A	In the lumbar g orly (dendritic) with the the di into the comm Ray neurons. In missure with R process forms n bles back on th from phasmid n

170	R4AL	MS	sensory neuron	tail - left lumbar ganglion	R(1-5)A	N/A	In the lumbar an anteriorly d with the the di into the comm put from R2AI the polL muscl ganglion: Ente R5BL, R7AL, process. Main may split in th rected, unbranc
171	R4AR	MS	sensory neuron	tail - right lumbar ganglion	R(1-5)A	N/A	In the lumbar g anteriorly direc the the distal e the commissure R2AR proximal and output to In the preanal R2BR, R7AR, I process with dis R4AL
172	R4BL	MS	sensory neuron	tail - left lumbar ganglion	Response	N/A	In the lumbar an anteriorly di with the the dis into the commi process. In the sure with R7BL directed, spiny rected branch. to LUA
173	R4BR	MS	sensory neuron	tail - right lumbar ganglion	Response	N/A	In the lumbar g anteriorly direc the the distal e the commissure cess. In the pre with R2BR, R directed, spiny rected branch.
174	R5AL	MS	sensory neuron	tail - left lumbar ganglion	R(1-5)A	N/A	In the lumbar g emanates from proximal to the processes, one c bing spiny and sure. This pro to various mus ganglion: Ente R6BL, R1BL. S put from Ray A

175	R5AR	MS	sensory neuron	tail - right lumbar ganglion	**R(1-5)A**	N/A	In the lumbar g emanates from mal to the CB, whose distal en cess has some i with body wall ters from comm splits to form a a longer anterio RayA neruons
176	R5BL	MS	sensory neuron	tail - left lumbar ganglion	**PVV**	N/A	In the lumbar dritic) process a anate from the asynaptic, whil one branch, wh from Ray A neu Ray A neurons commissure wit then splits to f rected processes
177	R5BR	MS	sensory neuron	tail - right lumbar ganglion	**PVV**	N/A	In the lumbar g directed proces emanate from t cess doubles ba sure. Output to preanal ganglio R5AR, R3BR, t processes and from AN3 and and Ray B neu
178	R6AL	MS	sensory neuron	tail - left lumbar ganglion	**PVV**	N/A	In the lumbar an anteriorly d The anterior p then runs into neurons, outpu muscle arm. In missure with R bifurcates to fo of the processes muscle, surroun tally and forms from several R and R7A

179	R6AR	MS	sensory neuron	tail - right lumbar ganglion	**PVV**	N/A	In the lumbar anteriorly direc distal portion then forms a fe commissure. In rons. In the pr with R2BR, R directed proces put/output wit rons. Main out
180	R6BL	MS	sensory neuron	tail - left lumbar ganglion	**PVV**	N/A	In the lumbar an anteriorly d with the the di into the commi near the comm from commissu splits to form Ray B neurons and EF3
181	R6BR	MS	sensory neuron	tail - right lumbar ganglion	**PVV**	N/A	In the lumbar g cess emanates sure proximal t commissure. Fe glion: long ante branches. Inpu R9BL
182	R7AL	MS	sensory neuron	tail - left lumbar ganglion	**PVV**	N/A	In the lumbar g anteriorly direc the the distal e the commissure posteriorly dire grtL muscle. In ganglion: Ente R4BL, R6AL, distally become several Ray neu other interneur
183	R7AR	MS	sensory neuron	tail - right lumbar ganglion	**PVV**	N/A	In the lumbar g anteriorly direc the the distal e the commissure Ray neuron inp ters from comm R4AR. Anterio with process ru Main input fro R6A and MS i

184	R7BL	MS	sensory neuron	tail - left lumbar ganglion	**PVV**	N/A	In the lumbar g anteriorly direc the the distal e the commissure and makes NM ganglion: Ente R4BL, R6AL, I is very spiny an directions of th Ray B neurons. rons
185	R7BR	MS	sensory neuron	tail - right lumbar ganglion	**PVV**	N/A	In the lumbar g anteriorly direc the the distal e the commissure and makes NM ganglion: Ente R2BR, R6AR, I is very spiny an directions of th neurons. Varied Ray B neurons
186	R8AL	MS	sensory neuron	tail - left lumbar ganglion	**Response**	N/A	In the lumbar g anteriorly direc the the distal en commissure. B ganglion via clo mid neurons in anteriorly direc MS sensory neu
187	R8AR	MS	sensory neuron	tail - right lumbar ganglion	**Response**	N/A	In the lumbar g anteriorly direc the the distal en commissure. B ganglion via clo comm. In the rected process PCA, output m
188	R8BL	MS	sensory neuron	tail - left lumbar ganglion	**Response**	N/A	In the lumbar two anteriorly d with the the di ning into the co naptic. Dendr R9BL. Enters p Few synapses i long, anteriorly spines at its te rons, mixed out

189	R8BR	MS	sensory neuron	tail - right lumbar ganglion		N/A	In the lumbar g riorly directed the distal end commissure. A terior process i longer (dendriti preanal ganglio in commissure In the preanal process, both of branch each at neurons, outpu
190	R9AL	MS	sensory neuron	tail - left lumbar ganglion	**Response**	N/A	In the lumbar two anteriorly d with the the dis into the commi sive input from naptic, and the form a posterio glion via cloaca the preanal gar with a couple n mainly from MS to MS and GS
191	R9AR	MS	sensory neuron	tail - right lumbar ganglion	**Response**	N/A	In the lumbar g emanates from directed branch the commissure from R9BR. En sure. Some syn Long, anteriorly mainly from MS LUA
192	R9BL	MS	sensory neuron	tail - left lumbar ganglion	**PVV**	N/A	In the lumbar an anteriorly d Dendritic proce commissure. C naptic. Enters Some synapses anteriorly direc both directions riorly on the rig Input mainly fr EF1 and EF2

193	R9BR	MS	sensory neuron	tail - right lumbar ganglion	PVV	N/A	In the lumbar rected process e imal to CB an R8BR and R9A commissure. O ganglion: Long branches. Inpu mainly to EF2
194	SPCL	MS	sensory/motor neuron	tail - left cloacal ganglion	Insemination	N/A	Makes NMJs w depressor musc
195	SPCR	MS	sensory/motor neuron	tail - right cloacal ganglion	Insemination	N/A	Makes NMJs w innervates the g
196	SPDL	MS	sensory neuron	tail - left cloacal ganglion	Locomotion	N/A	Runs in a bund anal ganglion a in the ventral c and ail muscles
197	SPDR	MS	sensory neuron	tail - right cloacal ganglion	Locomotion	N/A	Runs in a bund anal ganglion a in the ventral c body wall musc
198	SPVL	MS	sensory neuron	tail - left cloacal ganglion	Locomotion	N/A	Runs in a bund anal ganglion a in the ventral c neurons
199	SPVR	MS	sensory neuron	tail - right cloacal ganglion	Locomotion	N/A	Runs in a bund anal ganglion a in the ventral c neurons
200	VA08	GS	motor neuron	tail - ventral cord		22	Uncertain cell I tion
201	VA09	GS	motor neuron	tail - ventral cord	Locomotion	22	Uncertain cell I tion
202	VA10	GS	motor neuron	tail - ventral cord	Locomotion	21	Ventral portion tions with, and
203	VA11	GS	motor neuron	tail - preanal ganglion	Locomotion	21	Ventral portion tions with VD from AVA. Out
204	VA12	GS	motor neuron	tail - preanal ganglion	Locomotion	21	Ventral portion tions with VD from VB moto motor neurons
205	VB05	GS	motor neuron	tail - ventral cord	Locomotion	22	Uncertain cell I tion. Makes gap
206	VB06	GS	motor neuron	tail - ventral cord	Locomotion	22	Ventral portion tions with AVA AVA
207	VB07	GS	motor neuron	tail - ventral cord	Locomotion	21	Ventral portion tions with A,B A,B and D-type

208	VB08	GS	motor neuron	tail - ventral cord	**Locomotion**	**22**	Ventral portion tions with A,B Output to D-ty cles
209	VB09	GS	motor neuron	tail - ventral cord	**Locomotion**	**22**	Ventral portion tions with A an put to D-type r
210	VB10	GS	motor neuron	tail - ventral cord	**Locomotion**	**21**	Ventral portion tions with AVA D-type motor r
211	VB11	GS	motor neuron	tail - preanal ganglion	**Locomotion**	**21**	Ventral portion tions with AV NMJs with ail
212	VD09	GS	motor neuron	tail - ventral cord	**Locomotion**	**22**	Uncertain cell I tion. Extensive A and B-type r wall muscles
213	VD10	GS	motor neuron	tail - ventral cord	**Locomotion**	**22**	Ventral portion tions with D-ty B type motor muscles
214	VD11	GS	motor neuron	tail - preanal ganglion	**Locomotion**	**21**	Ventral portion tions with D-t Makes NMJs w
215	VD12	GS	motor neuron	tail - preanal ganglion	**Locomotion**	**21**	Makes gap junc portion input f input from SPV
216	VD13	GS	motor neuron	tail - preanal ganglion	**PVV**	**21**	Dorsal portion tral portion ma PVV. Makes N
217	link to map, synapse lists, circuit diagrams	GS or MS	neuron type	location of cell body	Module	Cluster	notes

4.2 Hermaphrodite C. elegans information

4.2.1 Neuron Centrality

5 MATLAB

5.1 Frequently Used Commands

Table 2: "Hub" neurons [11]

Name	AVAL	AVAR	AVBR	AVBL	AVER	AVEL
Degree	90	87	73	72	64	63

4.2.2 Ganglion Information

Glossary

Cluster Coefficient measures the density of connections among an average neuron's neighbors. [13].

$$C = \frac{1}{N}\sum_i C_i$$

$$C_i = \frac{2E(\mathcal{N}_i)}{k_i(k_i-1)}$$

where $E(\mathcal{N}_i)$ is the number of connections between neighbors of i, k_i is the number of neighbors of i, and C_i measures the density of connections in the neighborhood of neuron i (set $C_i = 1$ when $k_i = 1$). .

Dendrogram Tree diagram frequently used to illustrate the arrangement of the clusters produced by hierarchical clustering. .

Index of Qualitative Variation measures the heterogeneity of composition in a cluster. High IQV scores for a cluster indicate that the cluster is composed of various neuronal types or ganglionic neurons. .

Jaccard Coefficient The Jaccard similarity coefficientcient of two nodes i and j is

$$\frac{|neighbors(i) \cap neighbors(j)|}{|neighbors(i) \cup neighbors(j)|}$$

.

Local Motif Or network motif: "patterns of interconnections occuring in complex networks at numbers that are significantly higher than those in randomized networks. .

Modularity-based Community Detection From paper: Community structure in directed networks (doi: doi:10.1371/journal.pone.0037292) and Finding community structure in very large networks (Clauset et al) .

Participation Coefficient quantifies how extensively the connections of a neuron are distributed among different clusters. .

Power-law Degree Distributions Degree of distribution follows a power law (at least aymptotically): the fraction $P(k)$ of nodes in the network having k connections to other nodes goes for large values of k as

$$P(k) \sim k^{-\gamma}$$

A scale-free network follows such degree distribution. .

Simulated Annealing A method of stochastic optimization: Simulated Annealing & Metropolis Algorithm .

Survival Function The complement of cumulative distributio function. It captures the probability that the system will survive beyond a specified measure (time or others) .

T-test any statistical hypothesis test in which the test statistic follows a Student's t distribution if the null hypothesis is supported. .

Variation of Information between two partitions C and C' is defined as follows:

$$V(C, C') = V(X, Y) = H(X|Y) + H(Y|X),$$

where X and Y denote the vectors representing the cluster assignment of community divisions C and C', respectively. $H(X|Y)$ is the conditional entropy indicating the amount of additional information needed to describe C given C'. .

Within Module Weight evaluates how strongly a neuron is connected to other neurons within its cluster. .

References

[1] M Chalfie, J E Sulston, J G White, E Southgate, J N Thomson, and S Brenner. The neural circuit for touch sensitivity in caenorhabditis elegans. *The Journal of neuroscience: the official journal of the Society for Neuroscience*, 5(4):956–964, April 1985. PMID: 3981252.

[2] C. V. Gabel, H. Gabel, D. Pavlichin, A. Kao, D. A. Clark, and A. D. T. Samuel. Neural circuits mediate electrosensory behavior in caenorhabditis elegans. *Journal of Neuroscience*, 27(28):7586–7596, July 2007.

[3] A. L. Hodgkin and A. F. Huxley. A quantitative description of membrane current and its application to conduction and excitation in nerve. *Bulletin of Mathematical Biology*, 52(1-2):25–71, January 1990.

[4] Eduardo J. Izquierdo and Randall D. Beer. Connecting a connectome to behavior: An ensemble of neuroanatomical models of c. elegans klinotaxis. *PLoS Computational Biology*, 9(2):e1002890, February 2013.

[5] T. A. Jarrell, Y. Wang, A. E. Bloniarz, C. A. Brittin, M. Xu, J. N. Thomson, D. G. Albertson, D. H. Hall, and S. W. Emmons. The connectome of a decision-making neural network. *Science*, 337(6093):437–444, July 2012.

[6] Jon M. Kleinberg. Authoritative sources in a hyperlinked environment. *Journal of the ACM*, 46(5):604632, September 1999.

[7] Longzhuang Li, Yi Shang, and Wei Zhang. Improvement of HITS-based algorithms on web documents. In *Proceedings of the 11th International Conference on World Wide Web*, page 527535, Honolulu, HI, USA, 2002.

[8] Shawn R Lockery and Miriam B Goodman. The quest for action potentials in c. elegans neurons hits a plateau. *Nature Neuroscience*, 12(4):377–378, April 2009.

[9] Shawn R Lockery, Miriam B Goodman, and Serge Faumont. First report of action potentials in a c. elegans neuron is premature. *Nature Neuroscience*, 12(4):365–366, April 2009.

[10] Jerry E Mellem, Penelope J Brockie, David M Madsen, and Andres V Maricq. Action potentials contribute to neuronal signaling in c. elegans. *Nature Neuroscience*, 11(8):865–867, June 2008.

[11] Satoru Morita, Ken-ichi Oshio, Yuko Osana, Yasuhiro Funabashi, Kotaro Oka, and Kiyoshi Kawamura. Geometrical structure of the neuronal network of caenorhabditis elegans. *Physica A: Statistical Mechanics and its Applications*, 298(3-4):553–561, September 2001.

[12] Yunkyu Sohn, Myung-Kyu Choi, Yong-Yeol Ahn, Junho Lee, and Jaeseung Jeong. Topological cluster analysis reveals the systemic organization of the caenorhabditis elegans connectome. *PLoS Computational Biology*, 7(5):e1001139, May 2011.

[13] Lav R. Varshney, Beth L. Chen, Eric Paniagua, David H. Hall, and Dmitri B. Chklovskii. Structural properties of the caenorhabditis elegans neuronal network. *PLoS Computational Biology*, 7(2):e1001066, February 2011.

[14] J. G. White, E. Southgate, J. N. Thomson, and S. Brenner. The structure of the nervous system of the nematode caenorhabditis elegans. *Philosophical Transactions of the Royal Society B: Biological Sciences*, 314(1165):1–340, November 1986.

[15] Meng Xu, Travis A. Jarrell, Yi Wang, Steven J. Cook, David H. Hall, and Scott W. Emmons. Computer assisted assembly of connectomes from electron micrographs: Application to caenorhabditis elegans. *PLoS ONE*, 8(1):e54050, January 2013.